The chiral phase transition in charge ordered $1T$-$TiSe_2$

John-Paul Castellan[1], Stephan Rosenkranz[1], Ray Osborn[1], Qing'an Li[1],
K.E. Gray[1], Goran Karapetrov[1], J.P.C. Ruff[2], and Jasper van Wezel[1*]
[1] *Materials Science Division, Argonne National Laboratory, Argonne, IL 60439, USA.*
[2] *Advanced Photon Source, Argonne National Laboratory, Argonne, IL 60439, USA.*

It was recently discovered that the low temperature, charge ordered phase of $1T$-$TiSe_2$ has a chiral character. This unexpected chirality in a system described by only a scalar order parameter could be explained in a model where the inversion symmetry of the lattice is broken by the emergence of relative phase shifts between three charge density wave components. Here, we present experimental verification of the phase transition predicted by that theory, between non-chiral and chiral charge order. Employing both X-ray diffraction and electrical transport measurements, we find that the novel chiral phase transition in $1T$-$TiSe_2$ occurs ~ 7 K below its main charge ordering transition. We thus observe a hierarchy of charge ordered phases, leading from the high temperature normal state into the low temperature chiral state.

PACS numbers: 71.45.Lr,64.60.Ej,11.30.Rd

Introduction.—The modulation of electronic density, which emerges in charge ordered materials, may reduce the symmetry of the underlying lattice in various ways. Apart from the broken translational symmetry associated with the periodicity of the charge modulations, additional symmetries may be broken by the combination of the modified electron distribution and the atomic displacements resulting from electron-phonon coupling. These additional broken symmetries are key in understanding the material properties of many charge ordered systems. The breakdown of rotational symmetry in $2H$-$TaSe_2$, for example, is responsible for the presence of a reentrant phase transition under pressure [1]. Likewise, the broken inversion symmetry in the charge ordered phases of, for example, the rare-earth nickelates RNiO$_3$, renders those materials multiferroic [2].

Recently, it was discovered that the breakdown of inversion symmetry in the charge ordered phase of $1T$-$TiSe_2$ leads to the presence of a chiral structure at low temperatures [3–6]. In this phase, one charge density wave component out of the three that contribute to the charge order dominates in each atomic layer, and the rotation of the dominant direction of charge modulations as one progresses through consecutive atomic layers gives rise to a helical charge density distribution. While helical phases are common among spin-density wave systems, $1T$-$TiSe_2$ is one of only very few materials so far in which a chiral charge ordered phase has been suggested to exist [7, 8]. This discrepancy may be attributed to the scalar nature of its order parameter, which, unlike the vectorial order parameter of a spin-density wave, cannot be straightforwardly arranged in a helical fashion. A resolution to this problem was recently proposed, in which the chiral phase of $1T$-$TiSe_2$ is interpreted as a simultaneously charge and orbital ordered state [5].

The emergence of the chiral state in that model requires the presence of non-zero amplitudes for all three contributing charge density wave components, and therefore necessarily predicts a hierarchy of charge ordered phases as a function of temperature. Starting from the high-temperature uniform state, one should first undergo a phase transition into a non-chiral state in which all components of the charge order acquire non-zero amplitudes, but their phases remain equal. Only at a lower temperature is the chiral phase transition encountered, at which the relative phase differences become non-zero. These correspond to different spatial shifts of each charge density wave component along a helical axis, as well as a preferred occupation of given orbital orientations in each atomic layer [5, 9].

Here, we test the theoretical prediction that a hierarchy of phase transitions exists in $1T$-$TiSe_2$, using a combination of two complementary experimental probes. From the emergence of a novel peak in X-ray diffraction patterns and a concomitant anomaly in measurements of the electrical transport properties of the same sample, we conclude that the chiral charge order forms at ~ 186 K. The transition into the non-chiral charge density wave state is also clearly visible at ~ 193 K in both experiments. The analysis of these results shows them to be in good agreement with the theoretical model. They therefore constitute a direct observation of the predicted novel phase transition into a chiral charge ordered state.

Chiral Charge Order.—Titanium-diselenide is a quasi-two dimensional, layered material, in which hexagonal layers of Ti are sandwiched between similar layers of Se, and individual sandwiches are separated from each other by a large van der Waals gap. Its band structure has a small (positive or negative) indirect gap of the order of 150 meV or less [10, 11]. The top of the predominantly Se-4p valence band is located at the center of the first Brillouin zone, while the bottom of the Ti-3d conduction band lies at the zone boundaries. Although the nesting between these two bands is poor at best [12], $1T$-$TiSe_2$ is observed to undergo a phase transition at ~ 200 K in which a commensurate, 2x2x2 charge density wave forms, accompanied by a periodic lattice distortion.

The mechanism underlying the charge density wave transition is still heavily debated [13–16]. Regardless of what drives the formation of this charge order, however, it is clear that the charge density modulation consists of three distinct components. The wave vector of each component is given by one

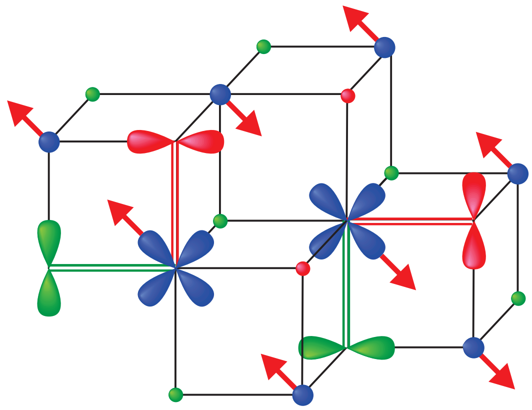

FIG. 1: (Color online) Schematic depiction of one of the charge density wave components in *1T*-$TiSe_2$. A single layer of Ti atoms (large and blue) is shown sandwiched between two layers of Se atoms (smaller, red and green). The atomic displacements of the Ti atoms are indicated by red arrows. These displacements result from the transfer of electronic weight between particular Ti-3d and Se-4p orbitals, which are shown explicitly for two of the Ti atoms and their Se neighbors. A non-zero, positive (or negative) phase shift in this charge density wave component corresponds to more charge being transferred along the bonds connecting Ti to the red upper Se layer than along the green lower bonds (or vice versa).

of the three vectors connecting the top of the Se band in the first Brillouin zone to the bottoms of the Ti bands on its edges. Because these bands all have distinct orbital characters, each charge density wave component corresponds to a charge transfer process between one particular Ti-3d orbital and two Se-4p orbitals. The resulting periodic lattice displacements of one of the components, are schematically indicated in Fig. 1. Superposing three such components, aligned along the three lattice directions of the hexagonal Ti-plane, gives rise a 2x2x2 lattice reconstruction.

If the three components are superposed without any relative phase differences, the resulting superstructure reproduces the non-chiral charge density wave state originally proposed for *1T*-$TiSe_2$ [17]. On the other hand, non-zero relative phase differences, corresponding to different spatial shifts of the charge density wave components along their propagation directions, result in a chiral lattice distortion [5]. Whether the chiral or the non-chiral state is energetically favorable, is determined by minimizing the Landau free energy. Writing the charge density wave order parameter as the sum of three complex parameters, $\psi_j = \psi_0 e^{i\vec{q}_j\cdot\vec{x}+\varphi_j}$, with equal amplitudes ψ_0 for all components, the free energy is given by

$$F = \psi_0^2 \left[a_0(T - T_{\mathrm{CDW}}) + a_1 \sum_j \cos(2\varphi_j) \right] + \psi_0^4 \left[b_0 + b_1 \sum_j \cos(2\varphi_j - 2\varphi_{j+1}) \right]. \quad (1)$$

Here a_0 and b_0 represent the combined effects of Coulomb interaction and the competition between charge density wave components, while the terms a_1 and b_1 are the leading order Umklapp terms which signify the coupling between the electronic order parameter and the atomic lattice [5].

Minimizing the free energy with respect to the phase variables yields two possible solutions. Coming from the high temperature phase, the non-chiral state with $\varphi_1 = \varphi_2 = \varphi_3$ is first realized at $T = T_{\mathrm{CDW}}$, when the amplitude ψ_0 becomes non-zero. At a lower temperature $T_{\mathrm{Chiral}} < T_{\mathrm{CDW}}$, the differences between the three phase variables φ_j become non-zero, and the chiral charge order sets in at a second-order phase transition. In the absence of experimental estimates for the various Ginzburg-Landau parameters, it is impossible to make a quantitative prediction for T_{Chiral}. From the expression of Eq. (1) however, it can be seen that the difference between T_{Chiral} and T_{CDW} is proportional to a_1/a_0, and may thus be expected to be small [5].

X-ray diffraction.—To test the predicted existence of a phase transition between the non-chiral and chiral phases of *1T*-$TiSe_2$, we performed X-ray diffraction experiments. Single crystal samples of *1T*-$TiSe_2$ were prepared by the iodine vapor transport method [18]. The sample used for this study had dimensions of approximately 3x3x0.05 mm^3. It was mounted on the cold finger of a closed cycle displex and aligned on a Huber six-circle diffractometer. X-ray measurements utilizing area detectors on the sector 6-ID-D high energy station of the APS were performed in transmission geometry, using an incident photon energy of 75 keV. Detailed order parameter measurements of the charge ordered phase emerging at T_{CDW} were made using the superlattice reflection $[\frac{3}{2},\frac{3}{2},\frac{1}{2}]$. The three-dimensional integrated intensity of these scans is presented in Fig. 2.

To measure the onset of chiral order below T_{CDW}, we first used area detectors to map out large volumes of reciprocal space to search for evidence of the emerging chiral order. We discovered extra peaks in the low temperature maps at wave vectors of the form $[H+\frac{1}{2},K,0]$, with intensities ~ 50 times weaker than the primary Bragg reflections. We then did a detailed order parameter measurement of one of these peaks, located at the $[\frac{5}{2},1,0]$ superlattice reflection. The three-dimensional integrated intensity is presented in Fig. 2.

Notice that the periodicity of the charge modulations does not change upon entering the chiral phase. Nevertheless, the appearance of new peaks in the diffraction data at the onset of chiral order, may be expected for several reasons. First of all, the lattice distortions in the chiral phase change the space group of the atomic lattice from $P\bar{3}c1$ into $P2$, which implies that several symmetry-forbidden peaks in the non-chiral phase are now allowed. The intensity for these previously forbidden reflections however, is expected to be very small, as they scale with the atomic displacements. Within the resolution of our experiment, we were indeed not able to identify any of these types of peaks.

An alternative way in which new reflections may occur is because a peak position with very little weight in the non-chiral phase may acquire significant weight in the chiral state, due to the combined effect of small changes in lattice struc-

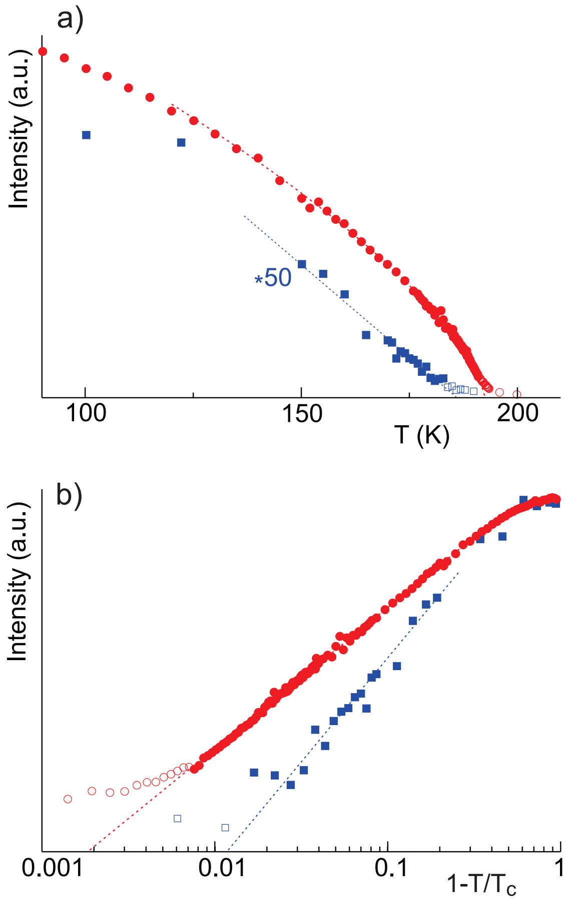

FIG. 2: (Color online) **a)** The integrated intensities of the superlattice reflections at [$\frac{3}{2}$,$\frac{3}{2}$,$\frac{1}{2}$] (upper, red curve) and [$\frac{5}{2}$,1,0] (lower, blue curve; amplified by a factor of 50). The former peak indicates a doubling of the unit cell in all crystallographic directions, and scales with the squared amplitude of the order parameter. The latter peak is present only in the chiral phase, and may be used as an order parameter for chirality. **b)** The same data on a log-log scale, as a function of reduced temperature. Here we used $T_C = T_{\rm CDW}$ for the upper, red curve, and $T_C = T_{\rm Chiral}$ for the lower, blue curve. The curve for the chiral order parameter is well described by a power-law with exponent $2\beta = 1.0$, while the fit for the red curve uses $2\beta = 0.68$. In both panels, the open symbols form a fluctuation tail, which extends beyond T_C.

ture and the onset of orbital order. The preferred occupation of a given set of orbitals on the different Ti and Se sites results in an anisotropic atomic structure factor, which can strongly affect the intensity of particular diffraction angles. The observed peaks at [$H+\frac{1}{2}$,K,0] are of this kind. We compared the evolution of one of these peak under decreasing temperature with that of one of the main charge density wave peaks.

As shown in Fig. 2a, the intensity of the [$\frac{3}{2}$,$\frac{3}{2}$,$\frac{1}{2}$] charge density wave peak first becomes non-zero at $T_{\rm CDW} = 193$ K. The small difference between this onset temperature and the accepted value of ~ 200 K for $T_{\rm CDW}$, may be attributed to a slight non-stoichiometric excess of Ti atoms, which is known to suppress the transition temperature in this compound [17]. The intensity of this peak is expected to be proportional to the squared amplitude of the charge density wave order parameter. The intensity of the reflection at [$\frac{5}{2}$,1,0] on the other hand, remains zero below the onset temperature $T_{\rm CDW}$, and begins to gain intensity only at the lower temperature $T_{\rm Chiral} = 186$ K, which we identify as the onset temperature of the chiral charge ordered phase.

The evolution of the two peak intensities with decreasing temperature can be clearly seen in Fig. 2b to be significantly different. The intensity of the main charge density wave peak close to $T_{\rm CDW}$ is best fitted by the power law $I = I_0(1-T/T_{\rm CDW})^{2\beta}$, with $2\beta \simeq 0.68$. The intensity of the peak related to the chiral order on the other hand, is well described by a power law with exponent $2\beta \simeq 1.0$. The difference between these critical exponents directly signifies a different origin for the types of order underlying the peak formation, and precludes the possibility that both peaks correspond to the same transition.

Electrical Transport.—Because the onset of the chiral charge density wave, and its corresponding orbital ordering, may be expected to affect the transport properties as well as the equilibrium lattice structure, we also performed detailed measurements of the principal components of the resistivity. In order to correctly determine both the resistivity along the c-axis, ρ_c, and in the ab-plane, ρ_{ab}, in a layered material like *1T*-$TiSe_2$, traditional four-terminal methods [19] may be inadequate and/or unreliable for single crystals, especially if the conductance anisotropy is large. This problem is easily overcome by a six-terminal method that uses a single crystal in a rectangular shape [20]. We employed four parallel Au stripes for electrical contacts, that were sputtered onto each c-axis-normal surface, perpendicular to the longest in-plane dimension of the crystal. The current was injected through the outermost contacts of one surface and voltages were measured across the innermost contacts of each surface. The Laplace equation was solved and inverted to get ρ_{ab} and ρ_c from the measured voltages [20, 21]. This method also allows a test of sample homogeneity by permuting the electrodes used for current and voltage [22].

The principle components of the resistivity for the same *1T*-$TiSe_2$ crystal used in the X-ray diffraction studies, are shown in Fig. 3a. The maximum variation upon permuting the electrodes is less than 5 %, implying a high degree of homogeneity. The temperature profiles of ρ_{ab} and ρ_c are also almost identical although their absolute values differ by an anisotropy factor of ~ 575. Each resistivity component exhibits a maximum close to 168 K. This maximum has been previously suggested to arise from an initial decrease in the density of available carriers, caused by the opening of a gap in the charge ordered phase, which is overtaken at lower temperatures by both the decrease of scattering channels due to the developing order, and an increase in density of states due to the downward shift of the conduction band minimum below $T_{\rm CDW}$ [23]. The position of the maximum thus does not coincide with the charge ordering transition. Instead, Di Salvo et al. found that a discontinuity in $d\rho/dT$ matches the onset of

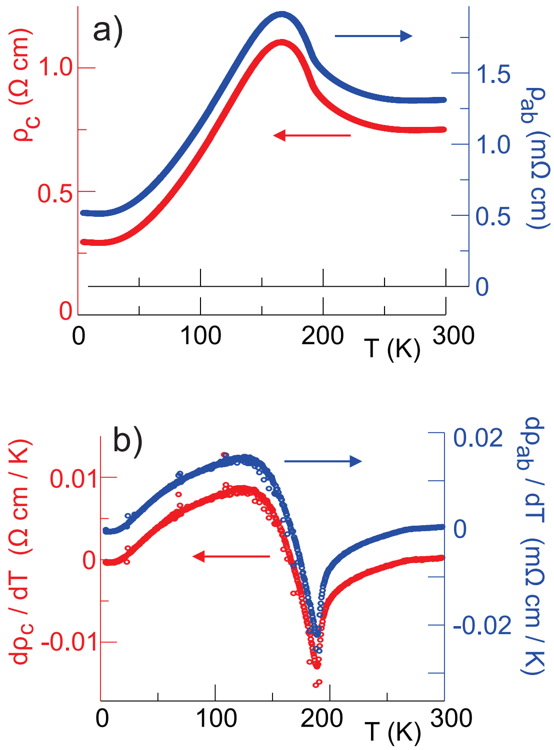

FIG. 3: (Color online) **a)** The variation of the two principal components of resistivity with temperature. The curves are offset in the vertical direction to distinguish them from each other. Notice that the scales for the two curves differ by a factor of ~ 575. **b)** The derivatives of both curves, which display sharp minima at the temperature T_{CDW}, where the amplitude of the (non-chiral) charge density wave first becomes non-zero.

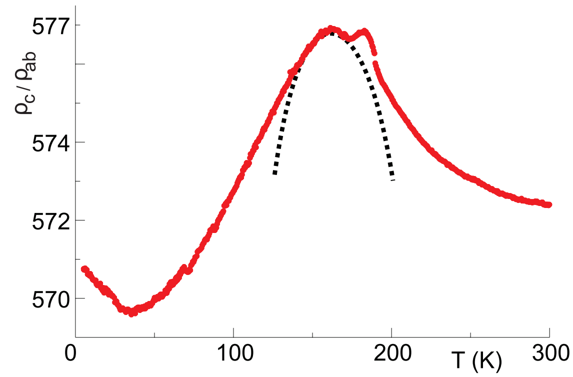

FIG. 4: (Color online) The anisotropy in resistivity ρ_c/ρ_{ab} as a function of temperature. Although the variation in anisotropy is only ~ 1.5 %, and thus small compared to the variation in overall resistivity, the sharp break at 183 K can be clearly identified. The change in anisotropy at this temperature indicates the onset of the chiral charge density wave. The associated orbital order is expected to affect the anisotropy of the scattering rates, and results in a sharp increase of the resistivity anisotropy. The broad feature centered at 161 K follows from the presence of broad maxima in $\rho_c(T)$ and $\rho_{ab}(T)$, and does not signify an additional transition. This effect is modeled by the dotted curve, which results from fitting the two peaks in Fig. 3a to simple parabolic functions.

the charge ordered superlattice as determined by neutron scattering [17], and this finding is confirmed in our data. Fig. 3b shows $d\rho_c/dT$ and $d\rho_{ab}/dT$ to be virtually coincident after scaling by the anisotropy, and the common discontinuity at 191 K matches closely the onset of the x-ray diffraction peak associated with the main charge order (see Fig. 2a).

The small variations in the resistivity anisotropy ρ_c/ρ_{ab}, are shown in Fig. 4. Interestingly, while $\rho(T)$ in Fig. 3a varies by more than a factor of three, the temperature variation of anisotropy is significantly smaller at only ~ 1.5 %. This observation agrees with the suggestion that the overall temperature dependence of $\rho(T)$ is determined primarily by the evolution of the carrier density [23], while the variations in anisotropy are determined by the temperature dependence of the scattering, which evidently plays a much smaller role. The anisotropy exhibits a sharp peak at 183 K and a relatively broad maximum centered at 161 K. The latter feature is a reflection of the slight differences in position and height of the maxima in $\rho_c(T)$ and $\rho_{ab}(T)$, and does not signify a qualitative change in physics. It can be modeled by fitting the two peaks of Fig. 3a to simple parabolas, which results in the anisotropy indicated by the dotted curve in Fig. 4. The sharp feature at 183 K on the other hand, matches the transition temperature for the chiral charge ordered state identified by the X-ray diffraction experiments (see Fig. 2a). Such a break in the temperature dependence of the anisotropy is most naturally attributed to a corresponding change in the anisotropy of scattering rates. Such an effect may be expected to occur at the onset of the chiral phase, due to the redistribution of electronic weight between the various involved orbital components.

Conclusions.—We conclude that the chiral charge and orbital ordered phase, which was recently discovered in *1T*-$TiSe_2$, arises from the non-chiral charge ordered state at $T_{\mathrm{Chiral}} \simeq 186$ K. This observation of the transition temperature close to the overall onset temperature T_{CDW} of charge order, agrees well with the theoretical prediction based on a Ginzburg-Landau treatment of the chiral order [5]. To identify the chiral phase transition, we employ measurements of both X-ray diffraction and resistivity anisotropy on the same sample of *1T*-$TiSe_2$.

The onset of chiral charge density wave order, and its associated lattice distortions and orbital order, result in the emergence of a previously absent x-ray diffraction peak. The exponent describing the power-law thermal evolution of this diffraction peak is significantly different from that associated with peaks already present in the non-chiral phase. At the chiral phase transition, we also find a distinct peak in the resistivity anisotropy, which is suggested to be related to the redistribution of orbital weight as the chiral phase sets in.

The combination of both of these sets of observations establishes the novel type of phase transition between non-chiral and chiral charge order in *1T*-$TiSe_2$, in agreement with theoretical predictions.

Acknowledgements

Use of the Advanced Photon Source and the work at the Material Science Division of Argonne National Laboratory were supported by the U.S. Department of Energy (DOE) Basic Energy Sciences under Contract No. NE-AC02-06CH11357.

* Electronic address: jvanwezel@anl.gov

[1] P. B. Littlewood and T. M. Rice, Phys. Rev. Lett. **48**, 27 (1982).
[2] G. Giovannetti, S. Kumar, D. I. Khomskii, S. Picozzi, and J. van den Brink, Phys. Rev. Lett. **103**, 156401 (2009).
[3] J. Ishioka, Y. H. Liu, K. Shimatake, T. Kurosawa, K. Ichimura, Y. Toda, M. Oda, and S. Tanda, Phys. Rev. Lett. **105**, 176401 (2010).
[4] J. van Wezel and P. B. Littlewood, Physics **3**, 87 (2010).
[5] J. van Wezel, Europys. Lett. **96**, 67011 (2011).
[6] M. Iavarone, R. D. Capua, X. Zhang, M. Golalikhani, S. A. Moore, and G. Karapetrov, Phys. Rev. B **85**, 155103 (2012).
[7] I. Guillamon, H. Suderow, J. G. Rodrigo, S. Vieira, P. Rodiere, L. Cario, E. Navarro-Moratalla, C. Martí-Gastaldo, and E. Coronado, New J. Phys. **13**, 103020 (2011).
[8] J. van Wezel, Phys. Rev. B **85**, 35131 (2012).
[9] J. van Wezel, Physica B **407**, 1779 (2012).
[10] F. J. Di Salvo and J. Waszczak, Phys. Rev. B **17**, 3801 (1978).
[11] A. Zunger and A. Freeman, Phys. Rev. B **17**, 1839 (1978).
[12] K. Rossnagel, L. Kipp, and M. Skibowski, Phys. Rev. B **65**, 235101 (2002).
[13] K. Rosssnagel, J. Phys. Cond. Mat. **23**, 213001 (2011).
[14] H. Cercellier, C. Monney, F. Clerc, C. Battaglia, L. Despont, M. G. Garnier, H. Beck, P. Aebi, L. Patthey, H. Berger, et al., Phys. Rev. Lett. **99**, 146403 (2007).
[15] J. van Wezel, P. Nahai-Williamson, and S. S. Saxena, Phys. Rev. B **81**, 165109 (2010).
[16] F. Weber, S. Rosenkranz, J. P. Castellan, R. Osborn, G. Karapetrov, R. Hott, R. Heid, K. P. Bohnen, and A. Alatas, Phys. Rev. Lett. **107**, 266401 (2011).
[17] F. J. Di Salvo, D. Moncton, and J. Waszczak, Phys. Rev. B **14**, 4321 (1976).
[18] C. Oglesby, E. Bucher, C. Kloc, and H. Hohl, J. Cryst. Growth **289**, 137 (1994).
[19] T. Kimura, Y. Tomioka, H. Kuwahara, A. Asamitsu, M. Tamura, and Y. Tokura, Science **274**, 1698 (1996).
[20] R. Busch, H. Werthner, G. Kreiselmeyer, G. Saemann-Ischenko, and G. Ries, Phys. Rev. Lett. **69**, 522 (1992).
[21] Q. A. Li, K. E. Gray, and J. F. Mitchell, Phys. Rev. B **59**, 9357 (1999).
[22] Q. A. Li, K. E. Gray, H. Zheng, H. Claus, S. Rosenkranz, S. Ancona, R. Osborn, J. F. Mitchell, Y. Chen, and J. Lynn, Phys. Rev. Lett. **98**, 167201 (2007).
[23] C. Monney, E. F. Schwier, M. G. Garnier, N. Mariotti, C. Didiot, H. Beck, P. Aebi, H. Cercellier, J. Marcus, and C. Battaglia, Phys. Rev. B **81**, 155104 (2010).